The Effective Drag Coefficient for Evaluating Wind Stress over the Oceans

KEVIN E. TRENBERTH, WILLIAM G. LARGE AND JERRY G. OLSON

National Center for Atmospheric Research, Boulder, Colorado*

(Manuscript received 24 March 1989, in final form 17 July 1989)

ABSTRACT

Computations of the surface wind stress and pseudostress over the global oceans have been made using surface winds from the European Centre for Medium Range Weather Forecasts for 7 years. The drag coefficient is a function of wind speed and atmospheric stability, and the air density is computed for each observation. Assuming a constant density, the effective drag coefficient required to convert the pseudostress into a stress has been computed for each month of the year using several methods. Because the drag coefficient varies from day-to-day and with the seasons, the effective drag coefficient cannot be uniquely defined and is a useful concept if only the very gross characteristics of the field are of interest and errors of the order of 10% are tolerable. Even then, the spatial and seasonal variations in C_D must be taken into account, and occasionally the wind stress may be greatly in error.

1. Introduction

Interactions between the atmosphere and the ocean are very important in the climate system. In this paper the main focus is on the surface momentum flux, or wind stress, by which the atmospheric winds drive oceanic currents so that the ocean acts as a sink for atmospheric momentum. Fluxes of heat and moisture are also important, and all three fluxes depend greatly upon the surface winds. The exchanges are most commonly parameterized using bulk aerodynamic formulae.

For the surface wind stress τ the bulk formulation is

$$\tau = [\tau_x, \tau_y] = \rho C_D V[u, v] \qquad (1)$$

where the surface wind (nominally at 10 m) is assumed to be parallel to the stress vector, with components $[u, v]$ and magnitude V (= wind speed). The density of surface air is ρ, C_D is the drag coefficient and the speed of the water is assumed negligible compared with the wind speed. Other nondimensional transfer coefficients C_T, the Stanton number for heat and C_E, the Dalton number for moisture should vary as $(C_D)^{1/2}$ (e.g., see Large and Pond 1982) but often they are assumed equal to C_D.

From (1) the magnitude of the stress is $|\tau| = \rho C_D V^2$, which serves as a useful definition of C_D. For instance, many estimates of C_D have been computed as the ratio of the directly measured Reynolds stress to the square of the wind speed (e.g., Large and Pond 1981). Often, through averaging, a single constant drag coefficient has been determined, which has the advantage of simplicity. But it is apparent from both theory and observations that all the exchange coefficients in fact depend on wind speed and atmospheric stability (Liu et al. 1979; Large and Pond 1981, 1982). The equivalent neutral drag coefficient, $C_N(V)$, is therefore commonly formulated as a function of wind speed, and

$$C_D = C_D(V, \sigma) = C_N(V) f(\sigma) \qquad (2)$$

where $f(\sigma)$ is a semiempirical function of the stability parameter σ (see Large and Pond 1982). Nevertheless, the experimental measurements are always difficult to obtain and a considerable scatter exists in most experimental results that compute C_D, leaving considerable uncertainty as to its true values as a function of the bulk parameters.

Partially because of these uncertainties in C_D and also because it has been claimed that for low frequency fluctuations (periods > 10 days) C_D = constant (Willebrand 1978; Goldenberg and O'Brien 1981), it has become common to compute a quantity called the pseudostress $\mathbf{P}$, given by

$$\mathbf{P} = [P_x, P_y] = V[u, v]; \qquad (3)$$

see Goldenberg and O'Brien (1981) and Servain and Legler (1986), for example. Note that $|\mathbf{P}| = V^2$. The implicit assumption is that surface air density is reasonably constant and that an effective drag coefficient $\hat{C}_D$ can then be used to convert $\mathbf{P}$ into τ, i.e.,

$$\rho_0 \hat{C}_D \mathbf{P} = \tau \qquad (4)$$

* The National Center for Atmospheric Research is sponsored by the National Science Foundation.

Corresponding author address: Dr. Kevin E. Trenberth, NCAR, P.O. Box 3000, Boulder, Colorado 80307-3000.

© 1989 American Meteorological Society

Unauthenticated | Downloaded 05/30/23 01:09 AM UTC

where ρ_0 is a constant density, often assigned 1.2 kg m^{-3}. For individual observations $\hat{C}_D$ differs from C_D by the factor ρ/ρ_0 which varies from ~0.97 at 30°C to 1.08 at 0°C. Additional complications arise when the pseudostress is averaged.

A project to compute a new global wind stress climatology incorporating the full variability of ρ, C_D and wind has been undertaken, and complete results are presented in Trenberth et al. (1989). As well as long-term means of wind stress, wind stress curl, and Sverdrup transport, the interannual variability is examined, and the means are compared with those of previous studies. The purpose of this paper is to examine how the resulting mean wind stress relates to the averaged pseudostress and whether the latter is really a useful concept. In other words, can a meaningful effective drag coefficient be defined? We are also interested in how constant in space and time the effective drag coefficient really is.

2. Data

Seven years (1980–86) of monthly mean wind stresses have been computed on a 2.5° × 2.5° grid based upon twice-daily 1000 mb wind analyses from the European Centre for Medium Range Weather Forecasts (ECMWF). The suitability of these data for such a purpose is addressed in detail in Trenberth et al. (1989).

The advantage of the analyses is that they provide much better coverage and temporal sampling over much of the world's oceans, especially in the Southern Hemisphere, than conventional ship data alone. Since the analysis method uses four-dimensional data assimilation, the surface wind analysis fully incorporates all the sea level pressure measurements, from buoys for instance, through a sophisticated variant of the geostrophic relation. The analyses also include relevant past information that has been effectively carried forward in time using the numerical weather prediction model. The disadvantage is that results depend entirely on the veracity of the analysis system in reproducing the true wind fields, and there are clearly problems in the tropics (see Trenberth et al. 1989). Although the 1000 mb level is not the surface, the manner of analysis of ship wind data at ECMWF prior to 9 September 1986 meant that the ship winds were effectively assigned to the 1000 mb level and the 1000 mb winds are the most appropriate ECMWF "surface" wind product prior to that date. Comparisons between ECMWF 1000 mb and observed wind speeds at Ocean Weather Ship Lima (57°N, 20°W) (Böttger 1982) for January to May 1982 reveal correlations of 0.87 and root-mean-square differences of 2.7 m s^{-1}, during a time when observed winds were up to 30 m s^{-1}.

3. Drag coefficients

The drag coefficient formulation used in the full wind stress computation

$$\begin{aligned} 10^3 C_N &= 0.49 + 0.065V \quad \text{for} \quad V > 10 \text{ m s}^{-1} \\ &= 1.14 \quad \text{for} \quad 3 \leqslant V \leqslant 10 \text{ m s}^{-1} \\ &= 0.62 + 1.56V^{-1} \quad \text{for} \quad V \leqslant 3 \text{ m s}^{-1} \end{aligned}$$

is based upon Large and Pond (1982) for $V > 3$ m s^{-1}. The lowest wind speed portion is an empirical fit to Dittmer (1977) and Schacher et al. (1981) at $V = 2$ m s^{-1} merged with the Large and Pond results at $V = 3$ m s^{-1} plus the notion that C_N should tend to ∞ as $V \to 0$. In applications of these formulas a lower limit on V of 1 m s^{-1} was set in computing C_N.

A stability dependence was also included to determine C_D from (2). Spatially varying climatological mean monthly values of air–sea temperature differences and surface humidity were computed using the Comprehensive Ocean–Atmosphere Data Set (COADS) and varied monthly but fixed within each month and from year to year. These variables, together with the ECMWF winds, were used[1] in the formula in Large and Pond (1982) to give the stability parameter σ at each grid point and every analysis time. The density was computed for each data point and time using the ECMWF values of temperature, pressure and moisture.

Ignoring a small dependence on relative humidity, the variation in drag coefficient as a function of wind speed and air–sea temperature difference is shown in Fig. 1. Because the pseudostresses and stresses were computed using the same averaging methods from the same data, the conclusions concerning the validity of their relationship should be robust. The most important point from Fig. 1 is the change in C_D with wind speed which, coupled with the temporal variations in density, potentially interferes with the simple relationship hoped for in (4).

Reasons for expecting differences between the effective drag coefficient and the mean drag coefficient can be illustrated using wind stress magnitude as an example. We partition the data to be averaged into means (overbars) and fluctuations (primes), such that $C_D = \bar{C}_D + C_D'$, $|\mathbf{P}| = \bar{P} + P'$, and $\rho = \bar{\rho} + \rho'$. Then the average wind stress magnitude, from (1), is

$$\overline{|\tau|} \approx \bar{\rho}\bar{C}_D\bar{P} + \bar{\rho}\overline{C_D'P'} + \overline{\rho' C_D'}\bar{P} \qquad (5)$$

where $\overline{C_D}\overline{\rho' P'}$ and the triple prime product terms are assumed negligible. The second term on the right-hand side of (5) will tend to be positive because the wind speed dependence of C_D will make $C_D' > 0$ when $P' > 0$, at least for winds above 10 m s^{-1} in the current formulation. Winds less than 3 m s^{-1} will have the opposite effect. It would also be expected that the third term on the right-hand side will tend to be positive because colder, more dense, air ($\rho' > 0$) will usually

[1] Monthly mean temperature and humidity differences, as given in Trenberth et al. (1989), were used because the ECMWF analyses do not include sea surface temperatures. Such a procedure is justified by Esbensen and Reynolds (1981).

Unauthenticated | Downloaded 05/30/23 01:09 AM UTC

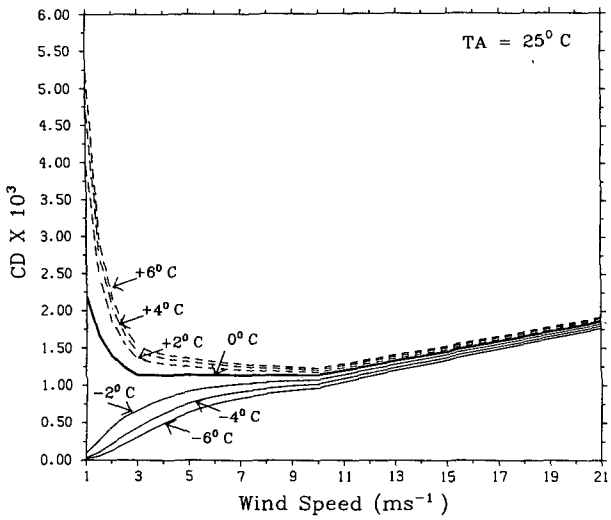

FIG. 1. Drag coefficient ($\times 10^3$) as a function of wind speed (m s^{-1}) for various air–sea temperature differences. Light solid lines, $\Delta T < 0$; dark solid lines $\Delta T = 0$; dashed lines, $\Delta T > 0$.

be associated with more unstable conditions over the warmer ocean, increasing C_D. Because we used climatological air–sea temperature differences in our calculations, however, the third term is not a factor here. Another consideration that further complicates matters is that stress is a vector and it is insufficient to deal only with the magnitude. Nevertheless, it appears that in general, and in our calculations, the effective drag coefficient should be expected to be greater than the mean drag coefficient. But the factors contributing to this effect will be highly variable in both time and space, depending, in particular, on the wind magnitude and steadiness.

Several possible alternative effective drag coefficients can be computed from (4) depending upon how time averages are taken and whether either of the two components or the magnitude of the stress is used. We have used six methods. There are $J = 7$ years of data and we define an overbar to be an individual monthly mean. We define $\bar{\bar{x}} = (1/J) \sum_{j=1}^{J} \bar{x}$ as the long-term mean over all years and days for each month. We then compute

$$\text{I.} \quad \rho_0 \hat{C}_D{}^1 = \overline{|\boldsymbol{\tau}|} / \overline{|\mathbf{P}|}$$

$$\text{II.} \quad \rho_0 \hat{C}_D{}^2 = |\bar{\bar{\boldsymbol{\tau}}}| / |\bar{\bar{\mathbf{P}}}|$$

$$\text{III.} \quad \rho_0 \hat{C}_D{}^3 = \bar{\bar{\tau}}_x / \bar{\bar{P}}_x$$

$$\text{IV.} \quad \rho_0 \hat{C}_D{}^4 = \bar{\bar{\tau}}_y / \bar{\bar{P}}_y$$

$$\text{V.} \quad \rho_0 \hat{C}_D{}^5 = (\overline{|\boldsymbol{\tau}|} / \overline{|\mathbf{P}|})$$

$$\text{VI.} \quad \rho_0 \hat{C}_D{}^6 = \overline{|\boldsymbol{\tau}|} / \overline{|\mathbf{P}|}.$$

Determination of $\hat{C}_D{}^1$ using method I would allow the scalar averaged wind stress to be estimated from the scalar averaged pseudostress. Here the property that wind stress is a squared quantity is taken into account, but not that it is a vector. The conversion of scalar averages into vector average magnitudes of wind stress depends on the wind steadiness, and hence on both time of year and geographical location.

For pseudostress to be useful, the most desirable quantity is $\hat{C}_D{}^2$, and it would be hoped that this would equal $\hat{C}_D{}^3$ and $\hat{C}_D{}^4$, implying that the stress and pseudostress vectors are parallel. Then vector averaged pseudostress could be readily converted into vector averaged stress components and magnitude. Unfortunately such is not the case and all three quantities are pathological because they go to infinity where the denominator goes to zero (which is not the same place where the numerator goes to zero). For the northern latitude weather ships, similar conversions of scalar, and vector averaged winds have been investigated by Esbensen and Reynolds (1981) and Marsden and Pond (1983), respectively. Here $\hat{C}_D{}^5$ is an attempt to improve upon $\hat{C}_D{}^2$ essentially by averaging over individual monthly mean values computed using method II; $\hat{C}_D{}^6$ is effectively the same thing but with the individual monthly $\hat{C}_D$ weighted by the pseudostress. The hope in method VI is that $|\bar{\mathbf{P}}|$ for a given month is not small in every one of the seven years. Only $\hat{C}_D{}^1$ is not badly behaved or very noisy somewhere, because the denominator is a scalar average of a positive definite quantity.

In general $\overline{|\boldsymbol{\tau}|} > |\bar{\bar{\boldsymbol{\tau}}}|$ and $\overline{|\mathbf{P}|} > |\bar{\bar{\mathbf{P}}}|$, but when their ratio is taken, as in methods I and II, the result is not obvious and $\hat{C}_D{}^1$ is not systematically larger or smaller than $\hat{C}_D{}^2$.

4. Results

Results are shown for methods I and II in Fig. 2 for January and Fig. 3 for July. Figures 4 and 5 present results for the other methods. Figures 6 and 7 show the ratio of several of the different estimates to provide an indication of where discrepancies greater than a few percent exist. All places where the denominator becomes small, thereby producing a bulls-eye, have been screened out on Figs. 2 to 5. In Figs. 6 and 7, the bulls-eyes have been retained but contours of only ±2.5, ±5, and ±10% are plotted to avoid the extremes. We consider all values between ±2.5% to be essentially unity and we consider only those values that differ by more than ±5%, which are stippled, to be significantly different from 1.

All methods have certain large scale features in common. Values of $\hat{C}_D \times 10^3$ are ~1.2 in the tropics and 1.6 or more at high latitudes with a clear seasonal variation and larger values in winter of both hemispheres. Since the minimum $10^3 C_N$ value is 1.14, effective drag coefficients near 1.2×10^{-3} are probably nearly the average coefficient, implying that the perturbation terms in (5) are small. A possible exception to this would be in very stable conditions and wind speeds less than 10 m s^{-1}. The area north of 35°N in

Unauthenticated | Downloaded 05/30/23 01:09 AM UTC

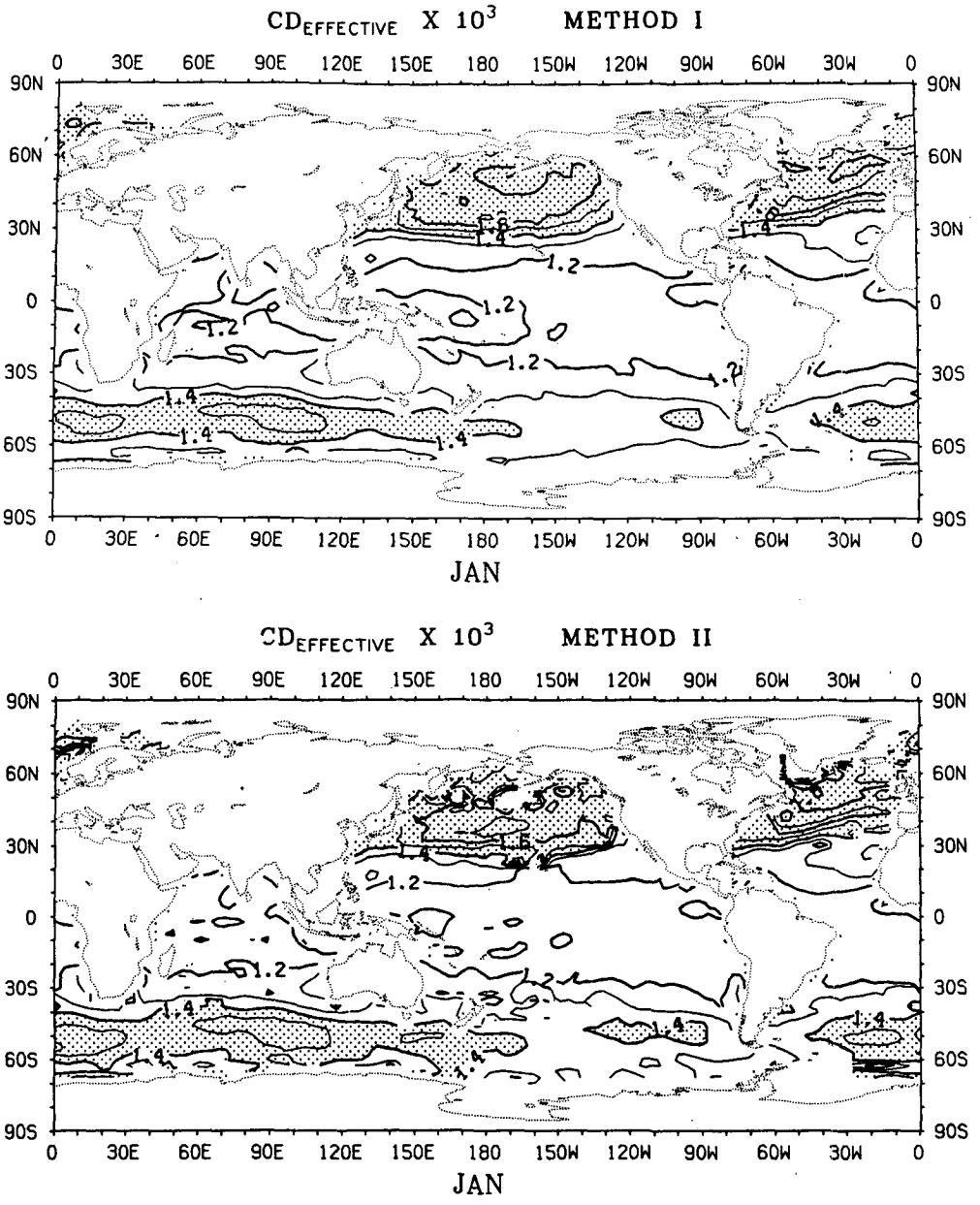

FIG. 2. Effective drag coefficient for methods I and II for January. Values greater than 1.4×10^{-3} have been stippled.

the Northern Hemisphere, is dominated by values greater than 1.6 in January but 1.2–1.3 in July. The January and July plots represent the annual cycle quite well. Because of the larger summer values in the Southern Hemisphere, the annual range is smaller. The results from method I are the most aesthetically pleasing because they are smoother and do not suffer from the pathology of some of the other values.

Bulls-eyes are not uncommon for $\hat{C}_D{}^2$ (Figs. 2 and 3) even in the tropics. At these points the effects of the unsteadiness in the wind has been to reduce the vector average pseudostress by a much greater amount than it has reduced the wind stress. Thus there are times and places where the use of pseudostress will result in vector wind stress estimates that are only a small fraction of the true value. In these instances, however, the vector averaged stresses are likely to be small so that the absolute differences should not be large even if the fractional error is big.

As noted earlier, for pseudostress to be a really useful concept, it is desirable to use a single $\hat{C}_D$ for each component. Because the total magnitude of the stress tends

Unauthenticated | Downloaded 05/30/23 01:09 AM UTC

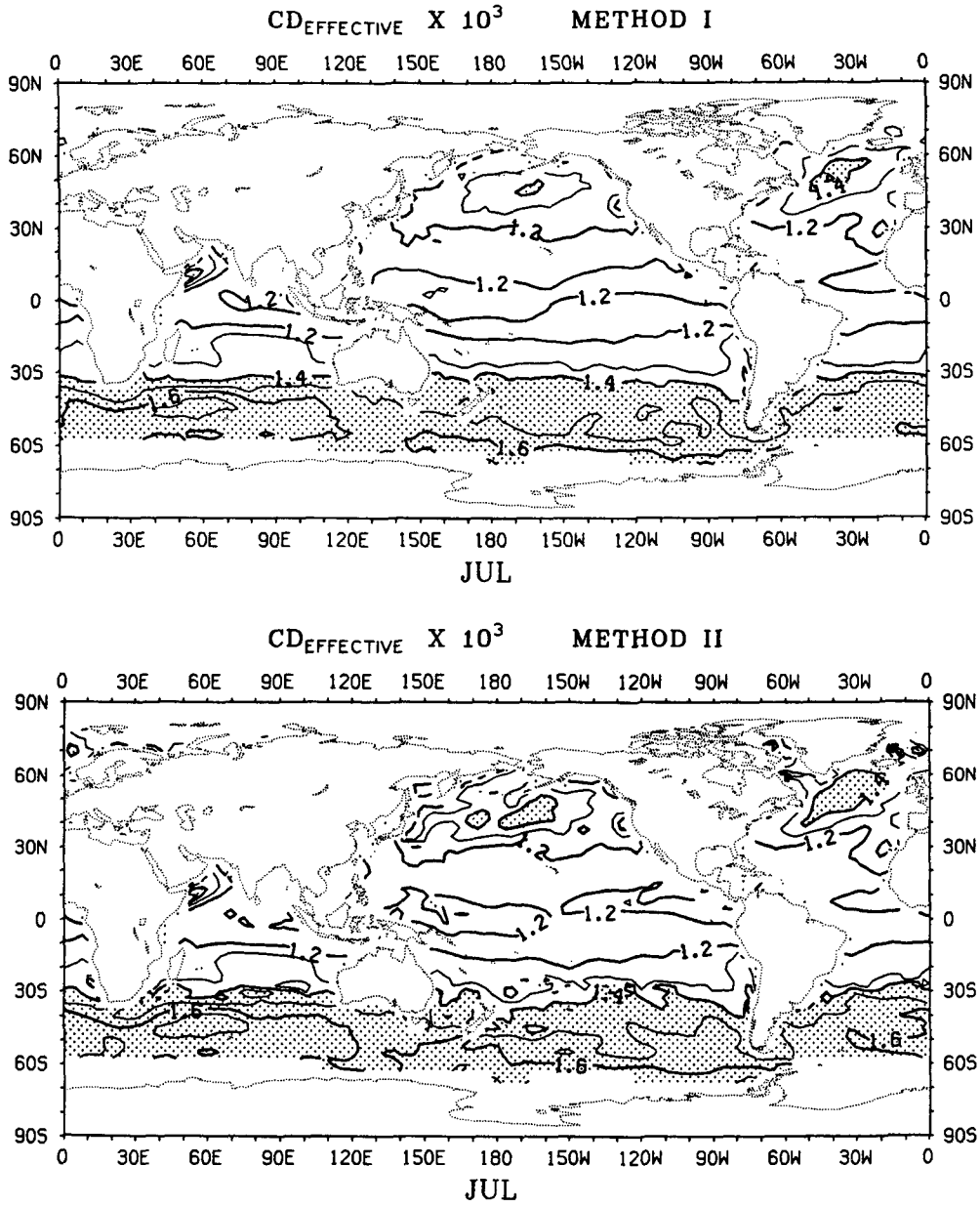

FIG. 3. Effective drag coefficient for methods I and II for July. Values greater than 1.4×10^{-3} have been stippled.

to be dominated by the x component, results for method II are quite similar to those from method III, but results from method IV are significantly different from both. As shown in Figs. 6 and 7, the differences in the resulting effective C_D exceed 5% over most of the domain outside of the tropics in both January and July. There are many more places in $\hat{C}_D{}^4$ where values become large producing bulls-eyes and a very noisy field. The interpretation of these results is that there are large portions of the global oceans where pseudo-stress is not quite parallel to the actual stress.

Results for method V are quite similar to method II but with the bulls-eyes damped. The field is still quite noisy. Largest differences occur in winter, especially near New Zealand. Further smoothing and improvement is apparent in method VI. Largest differences from method I occur near 60°S, in the North Pacific and, to a lesser extent, the North Atlantic in January, and in the North Pacific and near 30° and 50°S in July.

Typical values of the standard deviation of monthly means of $\hat{C}_D$ are ~5% of $\hat{C}_D$, with values reaching

Unauthenticated | Downloaded 05/30/23 01:09 AM UTC

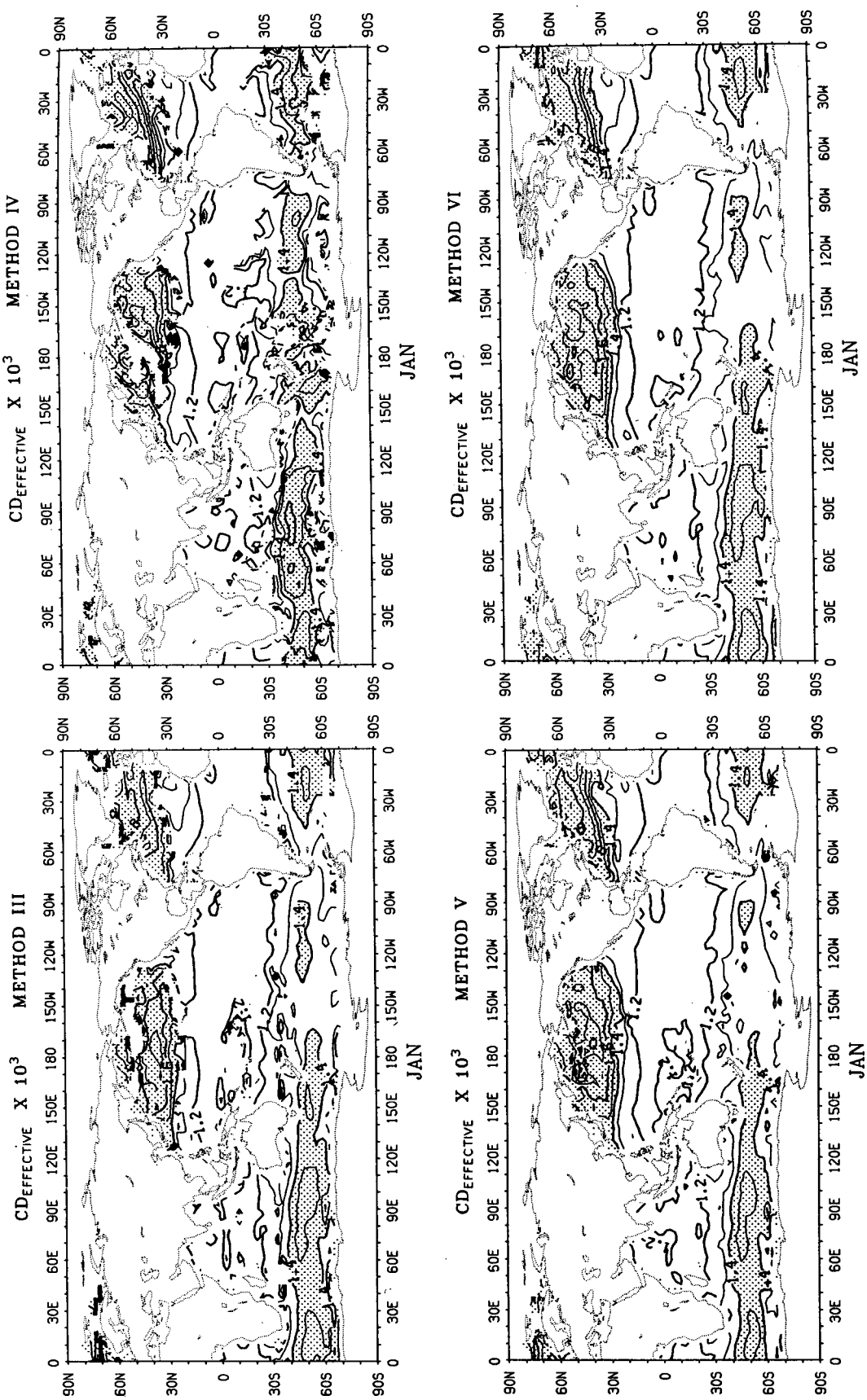

FIG. 4. Effective drag coefficient for methods III, IV, V and VI for January.

Unauthenticated | Downloaded 05/30/23 01:09 AM UTC

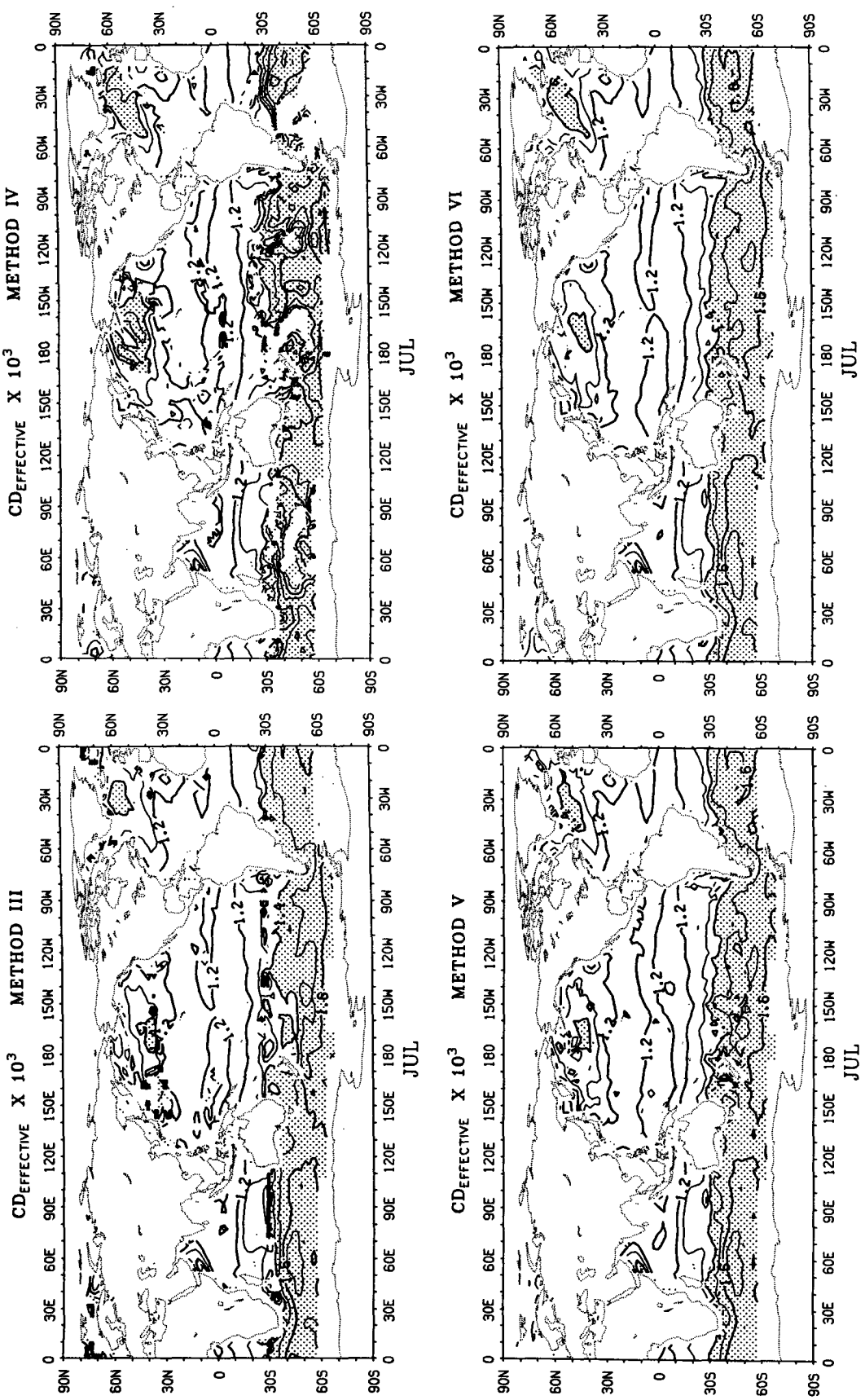

FIG. 5. Effective drag coefficient for methods III, IV, V and VI for July.

Unauthenticated | Downloaded 05/30/23 01:09 AM UTC

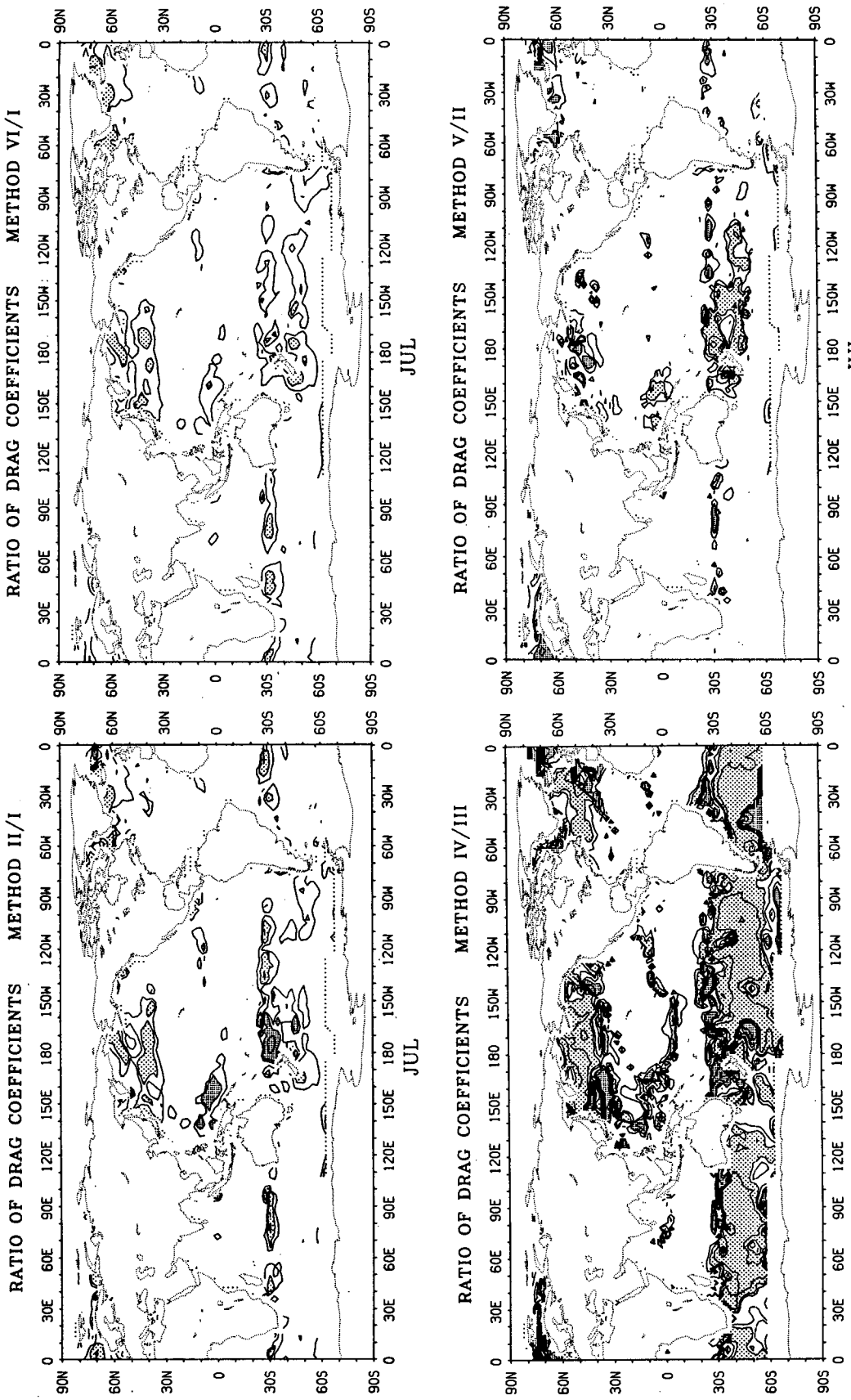

FIG. 6. Ratio of drag coefficients computed using differing methods for January. Contours are ±2.5, ±5, and ±10% from unity. Values less than 0.95 are densely stippled in a horizontal and vertical pattern and values greater than 1.05 are stippled in a cross pattern. Shown are ratios of methods II/I (top left), VI/I (top right), methods IV/III, and methods V/II.

Unauthenticated | Downloaded 05/30/23 01:09 AM UTC

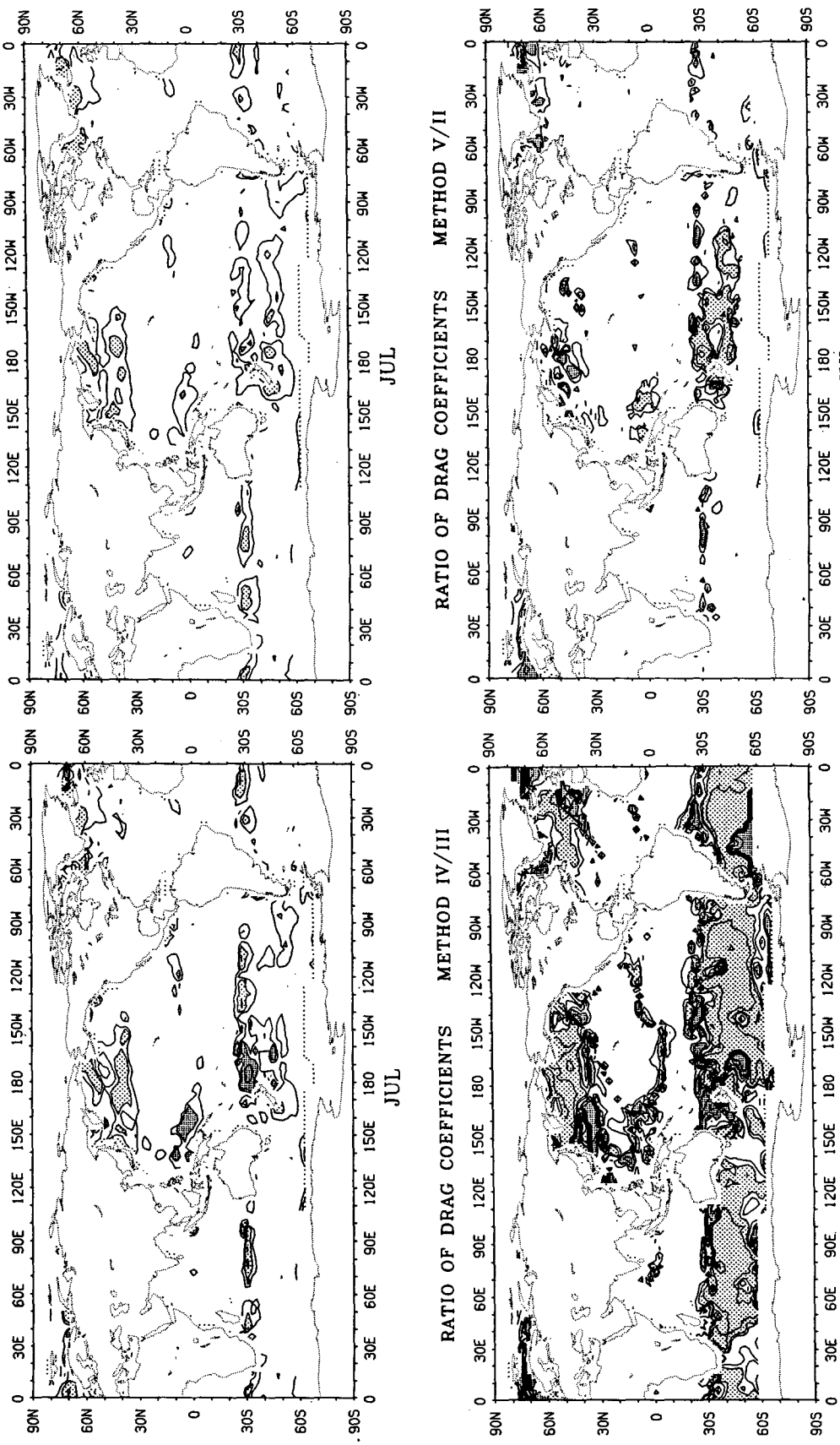

FIG. 7. Ratio of drag coefficients computed using differing methods for July. Contours are ±2.5, ±5, and ±10% from unity. Values less than 0.95 are densely stippled in a horizontal and vertical pattern and values greater than 1.05 are stippled in a cross pattern. Shown are ratios of methods II/I (top left), VI/I (top right), methods IV/III, and methods V/II.

Unauthenticated | Downloaded 05/30/23 01:09 AM UTC

$\sim 0.1 \times 10^{-3}$ in regions where $\hat{C}_D$ is $>1.4 \times 10^{-3}$. Consequently, interannual variability of $\hat{C}_D$ is not a major consideration.

It is worth noting the actual values of C_D that result from the calculations using the Large–Pond formulation. The details of the resulting wind stress climatology and comparisons with other results are presented in Trenberth et al. (1989), but we note that the values are considerably lower than used in most applications. At wind speeds of 20 m s^{-1} Bunker (1976), and Hellerman and Rosenstein (1983) use $C_N \sim 2.3 \times 10^{-3}$ versus 1.8×10^{-3} for Large and Pond. In the tropics, it has been common to assume values of $\hat{C}_D \sim 1.5 \times 10^{-3}$ (Wyrtki and Meyers 1976; Goldenberg and O'Brien 1981; Busalacchi and O'Brien 1980, 1981; O'Brien and Goldenberg 1982) or 1.4×10^{-3} (Philander et al. 1987), values that are 20%–30% larger than those estimated here. Most important, however, is that $\hat{C}_D$ varies substantially with space and time.

Many of these studies focus on the tropics and have used the concept of pseudostress in dealing with wind data. From our results in the tropics, it seems that most of the time the ratio of the different drag coefficients is within ±2.5% of unity, and thus the same coefficient could be used to compute all six stress-related quantities using any of the six methods. The main exception is in the tropical west Pacific north of the equator in July (Fig. 7), which is the time of the typhoon season. Apparently the relative steadiness of the trade winds and wind speeds of less than 10 m s^{-1} (for which the drag coefficient is constant, see Fig. 1) are responsible for this result over most of the tropics, whereas the variability in tropical storms upsets the relation in the western Pacific.

5. Conclusions

Because the drag coefficient depends upon wind speed and atmospheric stability, it varies from day to day and with the seasons. Consequently, the spatial and seasonal variations in the effective drag coefficient should be taken into account. Even then, there is no such unique quantity as $\hat{C}_D$ that can convert a pseudostress into the actual stress unless only the very gross characteristics of the field are of interest and errors of the order of 10% are tolerable from this factor. The possible exception is if applications are confined to the tropics. Owing to the temporal variability, however, there are times and places, even in the tropics, where averaging pseudostress distorts results too much to be compensated for with a spatially and temporally smooth effective drag coefficient.

The above conclusions should not be sensitive to the data used or the exact formulation of the drag coefficient because the same data were used to compute both the stress and the pseudostress, and a wind speed dependence is widely acknowledged (e.g., Bunker 1976; Hellerman and Rosenstein 1983). More importantly, relations such as the increase in drag coefficient with increasing pseudostress need to be captured.

Although the purpose of this paper has been to draw conclusions concerning the usefulness of the effective drag coefficient concept, we have also noted that the values assigned to the drag coefficient in previous studies are often larger than warranted.

Acknowledgments. The research of Trenberth and Olson is partially sponsored by the Tropical Oceans Global Atmosphere Project Office under Grant NA86AANRG0100. The data used were provided by ECMWF.

REFERENCES

Böttger, H., 1982. Local weather element guidance from the ECMWF forecasting system in the medium range. A verification study. *Seminar/Workshop 1982. Interpretation of numerical weather prediction products.* ECMWF. 417–441.

Bunker, A. F., 1976. Computations of surface energy flux and annual air–sea interaction cycles of the North Atlantic Ocean. *Mon. Wea. Rev.*, **104,** 1122–1140.

Busalacchi, A. J., and J. J. O'Brien, 1980. The seasonal variability in a model of the tropical Pacific. *J. Phys. Oceanogr.*, **10,** 1929–1951.

——, and ——, 1981. Interannual variability of the equatorial Pacific in the 1960's. *J. Geophys. Res.*, **86,** 10 901–10 907.

Dittmer, K., 1977. The hydrodynamic roughness of the sea surface at low wind speeds. *Meteor Forschungsergeb.*, **12,** 10–15.

Esbensen, S. K., and R. W. Reynolds, 1981. Estimating monthly mean-averaged air–sea transfers of heat and momentum using the bulk aerodynamic method. *J. Phys. Oceanogr.*, **11,** 457–465.

Goldenberg, S. B., and J. J. O'Brien, 1981. Time and space variability of the tropical Pacific wind stress. *Mon. Wea. Rev.*, **109,** 1190–1207.

Hellerman, S., and M. Rosenstein, 1983. Normal monthly wind stress over the world ocean with error estimates. *J. Phys. Oceanogr.*, **17,** 1093–1104.

Large, W. G., and S. Pond, 1981. Open ocean momentum flux measurements in moderate to strong winds. *J. Phys. Oceanogr.*, **11,** 324–336.

——, and ——, 1982. Sensible and latent heat flux measurements over the oceans. *J. Phys. Oceanogr.*, **12,** 464–482.

Liu, W. T., K. B. Katsaros and J. A. Businger, 1979. Bulk parameterization of air–sea exchanges of heat and water vapor including the molecular constraints at the interface. *J. Atmos. Sci.*, **36,** 1722–1735.

Marsden, R. F., and S. Pond, 1983. Synoptic estimates of air–sea fluxes. *J. Mar. Res.*, **41,** 349–373.

O'Brien, J. J., and S. B. Goldenberg, 1982. *Atlas of Tropical Pacific Wind Stress Climatology 1961–1970.* The Florida State University, 81 pp.

Philander, S. G. H., W. J. Hurlin and A. D. Seigel, 1987. Simulation of the seasonal cycle of the tropical Pacific Ocean. *J. Phys. Oceanogr.*, **17,** 1986–2002.

Schacher, G. E., K. L. Davidson, T. E. Houlihan and C. W. Fairall, 1981. Measurements of the rate of dissipation of turbulent kinetic energy, ϵ, over the ocean. *Bound.-Layer Meteor.*, **20,** 321–330.

Servain, J., and D. M. Legler, 1986. Empirical orthogonal function analyses of tropical Atlantic sea surface temperature and wind stress. *J. Geophys. Res.*, **91,** 14 181–14 191.

Trenberth, K. E., J. G. Olson and W. G. Large, 1989. A global ocean wind stress climatology based on ECMWF analyses. NCAR Tech. Note NCAR/TN-338+STR, 93 pp.

Willebrand, J., 1978. Temporal and spatial scales of the wind field over the North Pacific and North Atlantic. *J. Phys. Oceanogr.*, **8,** 1080–1094.

Wyrtki, K., and G. Meyers, 1976. The trade wind field over the Pacific Ocean. *J. Appl. Meteor.*, **15,** 698–704.

Unauthenticated | Downloaded 05/30/23 01:09 AM UTC